agronomy

MDPI

Article

Detection of QTL for High-Temperature Tolerance in Rice Using a High-Density Bin Map

Derun Huang [1], Zhenhua Zhang [1], Yeyang Fan [1], Shaoqing Tang [1], Jieyun Zhuang [1,*] and Yujun Zhu [1,2,*]

[1] State Key Laboratory of Rice Biology and Breeding, China National Rice Research Institute, Hangzhou 310006, China; huangderun@caas.cn (D.H.); zhangzhenhua@caas.cn (Z.Z.); fanyeyang@caas.cn (Y.F.); tangshaoqing@caas.cn (S.T.)
[2] Jiangxi Early-Reason Rice Research Center, China National Rice Research Institute, Pingxiang 337029, China
* Correspondence: zhuangjieyun@caas.cn (J.Z.); zhuyujun@caas.cn (Y.Z.)

Abstract: Rice is sensitive to high-temperature stress during almost all stages of growth and development. High-temperature stress has become one of the main factors restricting high yield and superior quality of rice. In this study, recombinant inbred lines (RILs) derived from an *indica* rice cross between two restorer lines were planted in two years. One sowing date was applied in 2019, and four sowing dates were set in 2020 according to the period of local high temperatures in recent years. Two traits closely related to high-temperature tolerance, heading date (HD), and spikelet fertility (SF) were measured. In each trial, the HD showed a bimodal distribution, whereas SF had a continuous and left-skewed distribution. QTL analysis was performed using a high-density bin map. For HD, a total of six QTL were detected. All of them correspond in position to the cloned genes, among which *qHD8* in the *DTH8*/*Ghd8* region showed the largest genetic effect. For SF, a total of eight QTL were detected. Five of them, *qSF1*, *qSF2*, *qSF3.1*, *qSF3.2*, and *qSF8*, showed high-temperature tolerance and had an important potential in rice breeding.

Keywords: rice; heading date; spikelet fertility; high-temperature tolerance; QTL

check for updates

Citation: Huang, D.; Zhang, Z.; Fan, Y.; Tang, S.; Zhuang, J.; Zhu, Y. Detection of QTL for High-Temperature Tolerance in Rice Using a High-Density Bin Map. *Agronomy* **2023**, *13*, 1582. https://doi.org/10.3390/agronomy13061582

Academic Editor: Chenggen Chu

Received: 16 May 2023
Revised: 9 June 2023
Accepted: 10 June 2023
Published: 12 June 2023

Copyright: © 2023 by the authors. Licensee MDPI, Basel, Switzerland. This article is an open access article distributed under the terms and conditions of the Creative Commons Attribution (CC BY) license (https://creativecommons.org/licenses/by/4.0/).

1. Introduction

Rice is one of the most important food crops in the world. More than half of the world's population takes rice as the main food source. Rice is sensitive to high-temperature stress (>35 °C) during almost all stages of growth and development [1]. At the reproductive stage, a temperature over 35 °C reduces pollen viability and increases the sterility of spikelets, resulting in a significant decline in rice yield [2–4]. At the early grain filling stage, high temperatures increase chalky rice percentage and chalkiness, and decrease milled rice percentage, resulting in a significant decline in rice appearance and milling quality [5,6]. Therefore, high-temperature stress has become one of the main factors restricting high yield and superior quality of rice.

Global climate change has caused the earth's surface temperature to rise in recent decades and is expected to increase 2 °C to 4 °C by 2050 [7]. Without effective adaptation, CO_2 fertilization, and genetic improvement, a one-degree Celsius increase in global mean temperature would, on average, reduce global yields of rice by 3.2% [8]. The Yangtze River region is the main rice planting area in China, where extremely high temperatures have appeared many times in recent years. In July and August of 2016 and 2017, the daily maximum temperature exceeding 35 °C in Wuhan, Hubei Province covered 26 d and 28 d, respectively, and that in Hangzhou, Zhejiang Province covered 34 d and 38 d, respectively (http://data.cma.cn/en, accessed on 20 March 2022). Since the 1970s, the rice planting pattern in China has gradually changed from double-season to single-season rice, and July–August is the reproductive development stage of single-season rice, which is vulnerable to high-temperature stress and reduced grain yield. The frequent occurrence of high temperatures for a long time indicates that the safe production of rice will become

more and more difficult. Thus, it is urgent to understand the genetic mechanism of high-temperature tolerance in rice.

Identification of quantitative trait loci (QTL) with high-temperature tolerance plays an important role in improving the heat tolerance of rice [9]. Many QTL with high-temperature tolerance were detected at various stages of development, such as the seeding [10], booting [11], flowering [12], and ripening stages [13], but only a few have been fine-mapped or cloned [14]. Three genes conferring heat tolerance at both vegetative and reproductive stages, *Thermo-tolerance 1* (*TT1*), *TT2*, and *TT3*, were isolated from the *Oryza glaberrima* accession CG14. *TT1* encodes a highly conserved 26S proteasome α2 subunit, which protects cells from heat stress through more efficient elimination of cytotoxic denatured proteins [15]. *TT2* encodes a Gγ submit, which regulates rice heat tolerance by participating in a calcium signal-mediated wax metabolism [16]. *TT3* encodes an E3 ubiquitin ligase TT3.1 and a chloroplast-localized membrane protein TT3.2, which enhances rice heat tolerance through cell membrane–chloroplast signal transduction [17]. In addition, *qHTT8*, a major QTL that controls high-temperature tolerance at the flowering stage, was detected in a heat-tolerant cultivar Huanghuazhan. Two annotated genes, *LOC_Os08g07010* and *LOC_Os08g07440*, were determined as candidate genes for *qHTT8* [4]. Another QTL, *qHTB1-1* controlling heat tolerance at the booting stage, was detected from a wild *Oryza rufipogon Griff* accession HHT4 and fine-mapped to a 47.1 kb region [18]. In addition to these QTL identified from natural variation populations, some genes related to heat tolerance were also identified through mutant and reverse genetics studies, such as *ERECTA* [19], *OsHTAs* [20], and *HSA1* [21]. Although great progress has been made in the identification and cloning of heat-tolerant genes in rice, the molecular mechanism of heat tolerance is still elusive, and more heat-tolerant genes need to be further explored.

Heading date (HD) and spikelet fertility (SF) are two key traits of rice variety improvement. HD is closely related to rice grain yield and quality [22,23] and is a key trait that determines the adaptability of rice planting areas and seasons [24]. Recent studies also suggested that traditional heading date genes in rice may have roles in stress response [23,25,26]. SF is influenced by both genetic and environmental factors and is the most unstable yield component of rice. In addition, SF is also an important evaluation index of high-temperature tolerance in rice [27]. Genetic analysis of HD and SF under high-temperature stress may find favorable alleles with high-temperature tolerance.

In this study, recombinant inbred lines (RILs) derived from an *indica* rice cross between two restorer lines of three-line hybrid rice were used to identify QTL for HD and SF that were related to high-temperature tolerance. For HD, a total of six QTL were detected. All of them correspond in position to the cloned genes, among which *qHD8* in the *DTH8*/*Ghd8* region showed the largest genetic effect. For SF, a total of eight QTL were detected. Five of them, *qSF1*, *qSF2*, *qSF3.1*, *qSF3.2*, and *qSF8*, showed high-temperature tolerance and had an important potential in rice breeding.

2. Materials and Methods

2.1. Rice Material and Field Experiment

One RIL population consisting of 256 lines was used in this study. It was constructed in our previous study [28] from an *indica* rice cross between two restorer lines of three-line hybrid rice, Dan 71 (D71) and Zhonghui 161 (ZH161).

The RIL population and its two parents were planted in the paddy field at the China National Rice Research Institute, Hangzhou, Zhejiang Province, China. They were tested for two years. In 2019, the sowing and transplanting date was 17 May and 10 June, respectively. In 2020, they were grown from May to November with four sowing dates according to the period of local high-temperature days in recent years. The sowing and transplanting dates were 19 May and 11 June for the 1st sowing (SD1), 26 May and 16 June for the 2nd sowing (SD2), 2 June and 21 June for the 3rd sowing (SD3), and 9 June and 28 June for the 4th sowing (SD4), respectively. In 2019, the trial followed a randomized complete block design with two replications. In 2020, the four trials were performed with no replication.

Each line was planted in a single row of 12 plants. The planting space was 16.7 cm between plants and 26.7 cm between rows. Filed management followed normal agricultural practice. In 2019, the daily maximum temperature exceeding 35 °C covered only 7 days. In 2020, 29 of the 31 days from 28 July to 27 August had a daily maximum temperature above 35 °C.

2.2. Phenotype Evaluation

HD and SF were measured in all trails. In 2019, HD was recorded for individual plants at the first panicle that emerged from the leaf sheath and averaged for each line. In 2020, HD for each line was recorded as days from sowing to the time when 50% of the 12 plants had emerged from the leaf sheath. At maturity, five plants of each line from the middle ten plants were harvested in bulk and measured for SF.

2.3. QTL Detection

A high-density linkage map consisting of 1246 genetic markers was previously constructed, which included 1219 bin markers, 22 SSR markers randomly located on 12 chromosomes, 3 STS markers for heading genes *Hd1*, *Hd2*, and *Ghd8*, and 2 STS markers for rice blast resistance genes *Pi9* and *Pi25*. The bin marker development was conducted by Guangzhou Genedenovo Biotechnology Co., Ltd. (Guangzhou, China) through genome-wide resequencing. The other markers were used to verify the genotype of the bin markers (Table S1). The linkage map was constructed using Mapmaker/Exp 3.0. It spanned 1798.1 cM, covering about 92.5% of the rice genome, and the average interval between adjacent markers was 1.5 cM [28]. QTL analysis was performed using QTL IciMapping 4.1 with the functionality of BIP (QTL mapping in the biparental populations). *LOD* thresholds were computed with 1000 permutation tests ($p < 0.05$) and used to declare a putative QTL [29]. QTL were named following the rule proposed by McCouch and CGSNL [30].

3. Results

3.1. Performance of HD and SF of the RILs

Descriptive statistics of HD and SF for the RILs and the average trait values of the two parents in each trial are presented in Table 1. In the RIL population, trait values of HD showed a bimodal distribution in all trials (Figure 1A,C–F), indicating the presence of major gene control for the variation. For SF, the trait values showed a continuous and left-skewed distribution in all trials (Figure 1B,G–J), indicating the presence of accumulative effects from multiple factors for decreasing SF.

Table 1. Performance of heading date and spikelet fertility in the D71/ZH161 RIL population.

Trait [a]	Trial [b]	Range	Mean ± SD	Skewness	Kurtosis	Parental Mean	
						D71	ZH161
HD (d)	2019	75.9–109.4	90.8 ± 8.2	0.03	−1.17	92.4	89.8
	2020-SD1	74.0–110.0	90.2 ± 9.0	0.09	−1.21	96.0	91.0
	2020-SD2	72.0–106.0	88.5 ± 9.0	0.02	−1.45	91.0	85.0
	2020-SD3	73.0–107.0	90.3 ± 9.3	0.13	−1.49	96.0	89.0
	2020-SD4	68.0–107.0	87.8 ± 9.4	0.04	−1.19	97.0	91.0
SF (%)	2019	55.1–95.1	83.9 ± 6.7	−1.00	1.44	76.2	91.8
	2020-SD1	55.9–96.1	85.5 ± 6.4	−1.38	2.85	62.7	95.4
	2020-SD2	63.3–96.1	87.7 ± 5.9	−1.43	2.46	68.9	94.9
	2020-SD3	50.1–97.0	84.9 ± 8.5	−1.30	1.94	79.1	96.1
	2020-SD4	38.3–96.5	82.4 ± 11.4	−1.25	1.34	60.7	92.0

[a] HD, heading date; SF, spikelet fertility. [b] Five trials were conducted, including one in 2019 with a sowing date on 17 May, and four in 2020 with sowing dates on 19 May (SD1), 26 May (SD2), 2 Jun (SD3), and 9 Jun (SD4).

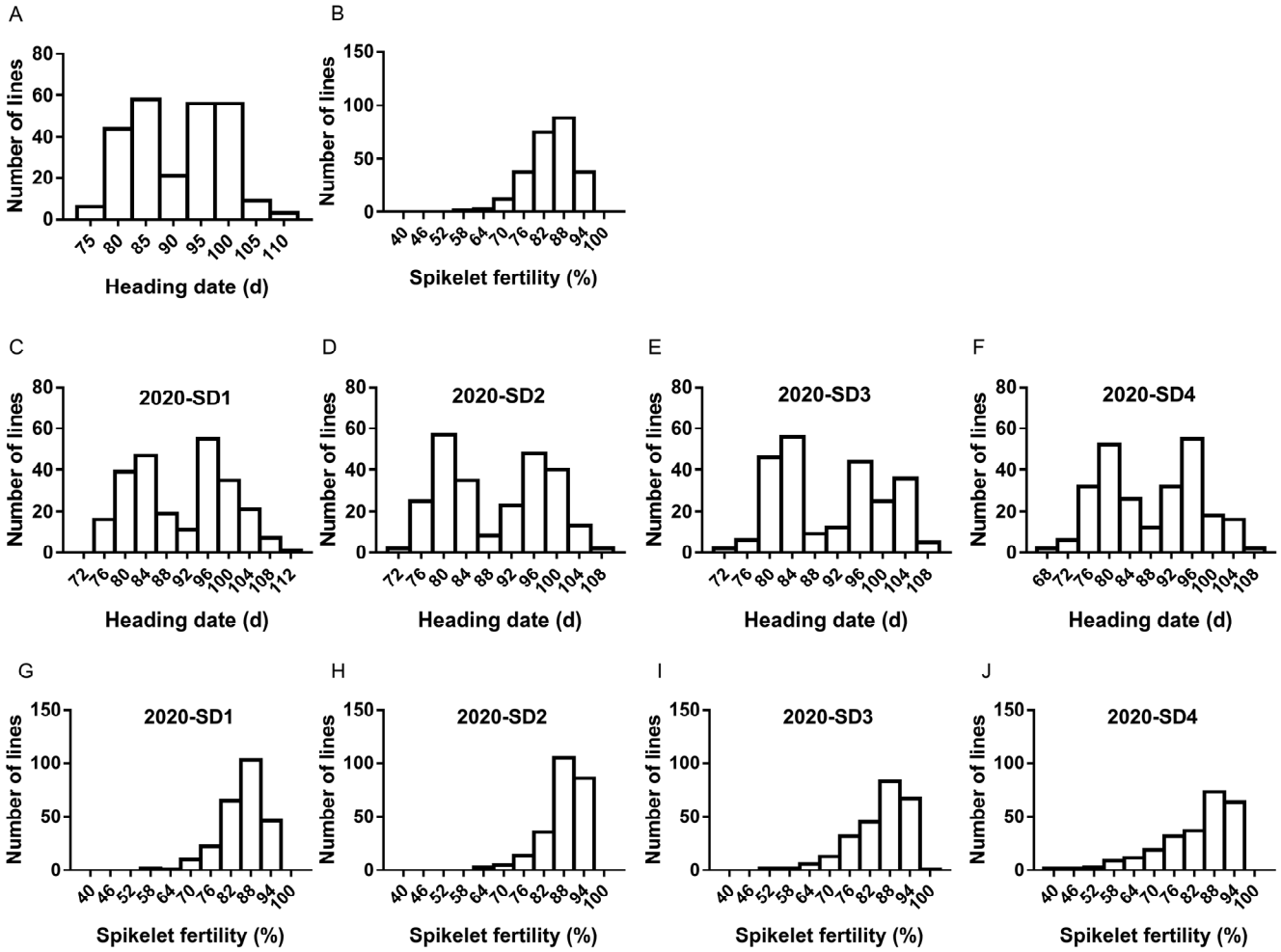

Figure 1. Distribution of heading date and spikelet fertility of the RILs in 2019 and 2020. (**A**,**B**) Heading date and spikelet fertility in 2019. (**C**–**F**) Heading date at four sowing dates in 2020. (**G**–**J**) Spikelet fertility on four sowing dates in 2020. SD1, SD2, SD3, and SD4 indicated the first, second, third, and fourth sowing dates, respectively.

HD (r = 0.9757; p < 0.0001) and SF (r = 0.3633; p < 0.0001) of the RILs had significant correlations between the two trials with similar sowing dates, i.e., the single-sowing trial in 2019 and the first trial in 2020. In addition, regression analysis showed that SF was hardly dependent on HD in these two trials, with R^2 values of 0.0150 and 0.0195 in 2019 and 2020, respectively. In the other three trials in 2020, the regression coefficients increased with the delay of the sowing date, becoming 0.0967, 0.3810, and 0.5939 on SD2, SD3, and SD4, respectively. A decrease in SF and an increase in HD was observed for a few RILs on SD1 and SD2 (Figure 2A,B), but it was evident on SD3 and SD4 (Figure 2C,D). As shown in Figure 2, the heading date corresponding to the sharp decrease in SF started one week after the high-temperature period. The decrease became more and more severe for 2–3 weeks until normal flowering of the RILs was completed. These results indicate that the early-middle phases of spikelet development are sensitive to high temperatures in the D71/ZH161 RIL population.

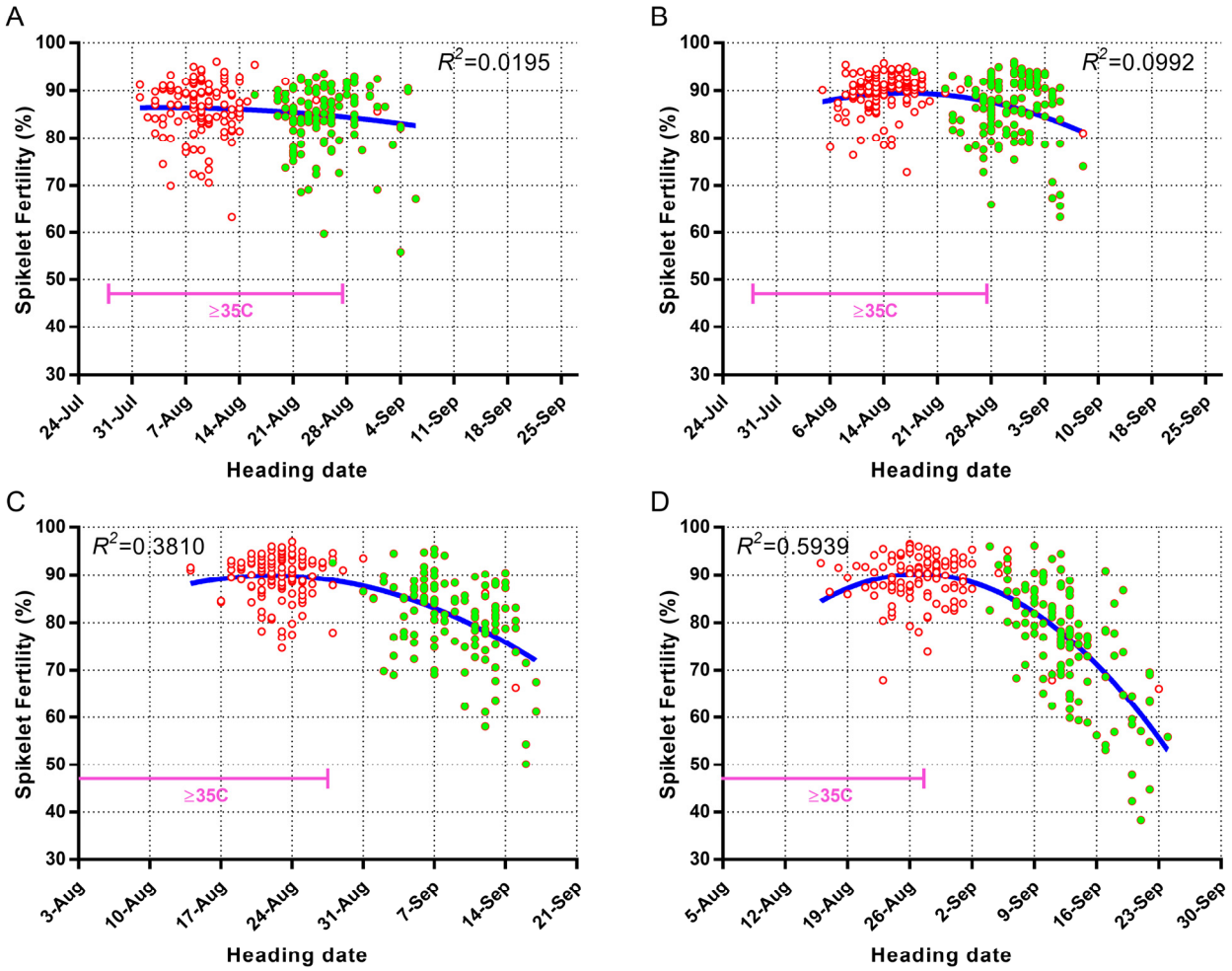

Figure 2. Correlation between heading date and spikelet fertility in 2020. (**A**), The first sowing. (**B**) The second sowing. (**C**). The third sowing. (**D**). The fourth sowing. The pink line indicates the period when the daily maximum temperature exceeded 35 °C. The green dots indicate subpopulation 1, which carried the Dan71 functional allele at the *DTH8* locus. The red dots indicate subpopulation 2, which carried the ZH161 nonfunctional allele at the *DTH8* locus.

3.2. QTL Detected for HD

With 1000 permutation tests ($p < 0.05$), the threshold of HD QTL in the five trials ranged from 1.7 to 3.4. To exclude false positive QTL, a score of 3.4 was set as the *LOD* threshold. Six QTL for HD were detected (Figure 3, Table 2), including one (*qHD1*) in 2019 and five (*qHD3*, *qHD5*, *qHD6*, *qHD7*, and *qHD8*) in both years. The QTL corresponds in position to the cloned gene *DTH8*/*Ghd8* [31,32], *qHD8*, explained a major proportion of the phenotypic variance in each of the five trials, ranging from 70.8% to 83.4%. Its additive effect ranged from 7.1 d to 8.3 d, and the allele for delaying the heading was derived from the female parent D71. Based on the genomic sequences of *DTH8* and genotypes of the gene marker Ei4334, D71 carries a functional allele and ZH161 carries a nonfunctional allele. Since *DTH8* functions to delay heading [31,32], the $DTH8^{D71}$ allele delay heading was expected.

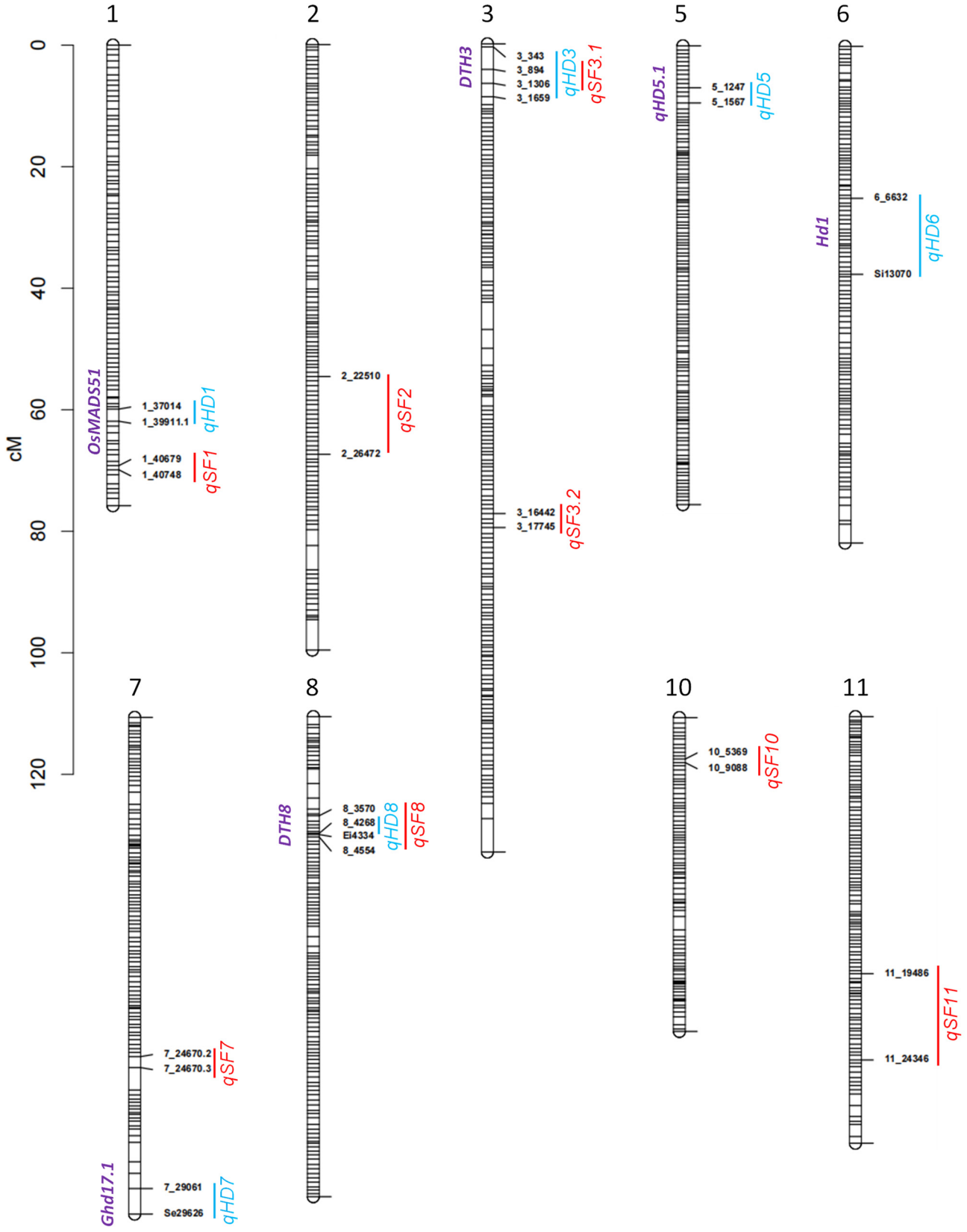

Figure 3. Chromosomal (numbered on the top) locations of QTL for heading date and spikelet fertility detected in the D71/ZH161 RIL population. HD, heading date (d); SF, spikelet fertility (%).

Table 2. QTL for heading date detected in the D71/ZH161 RIL population.

QTL	Interval [a]	Trial	*LOD*	*A* [b]	R^2 (%) [c]
qHD1	1_37014–1_39911	2019	3.4	−0.6	0.6
qHD3	3_343–3_1659	2019	15.6	1.5	2.9
		2020-SD1	10.3	1.3	1.8
		2020-SD2	11.3	1.5	2.6
		2020-SD3	7.2	1.3	1.9
		2020-SD4	8.3	1.6	2.9
qHD5	5_1247–5_1567	2019	3.7	0.7	0.6
		2020-SD1	18.3	1.8	3.6
qHD6	6_6632–Si13070 (6_13070)	2019	9.4	−1.1	1.6
		2020-SD1	6.9	−1.0	1.2
		2020-SD2	7.2	−1.2	1.6
		2020-SD3	8.1	−1.3	2.1
		2020-SD4	5.4	−1.3	1.9
qHD7	7_29061–Se29626 (7_29626)	2019	51.3	3.1	13.3
		2020-SD1	32.4	2.5	7.3
		2020-SD2	22.3	2.2	5.7
qHD8	8_4268–Ei4334 (8_4334)	2019	133.0	−7.1	70.8
		2020-SD1	123.3	−8.0	75.6
		2020-SD2	116.6	−8.1	78.1
		2020-SD3	108.5	−8.3	83.4
		2020-SD4	91.1	−8.2	76.5

[a] An interval is indicated by the two markers flanking the QTL. An SNP marker is named the chromosome No. followed by the physical position in kb. The physical positions of the three gene markers are shown in the parenthesis. [b] *A*, additive effect of replacing a maternal allele with a paternal allele. Positive values indicate that alleles from ZH161 are in the direction of increasing the trait score, and negative values indicate that alleles from D71 are in the direction of increasing the score. [c] R^2, the proportion of phenotypic variance explained by the QTL effect.

Five of the other QTL, *qHD1*, *qHD3*, *qHD5*, *qHD6*, and *qHD7*, correspond in position to the cloned genes *OsMADS51* [33], *DTH3* [34], *Hd1* [35], *qHd5* [36], and *Ghd7.1* [37], respectively. Compared with the D71 alleles, the ZH161 alleles promote heading at *qHD1* and *qHD6*, and delay heading at *qHD3*, *qHD5*, and *qHD7* (Table 2).

3.3. QTL Detected for SF

As described above, SF of the RILs was significantly associated with HD under high-temperature stress, and a major proportion of HD variance was explained by *qHD8*/*DTH8*. To investigate SF with and without the presence of *DTH8* variation, we divided the D71/ZH161 population into two subpopulations. Sub1 consisted of 133 lines carrying the functional $DTH8^{D71}$ allele, and Sub2 contained 120 lines carrying the non-functional $DTH8^{ZH161}$ allele. QTL analysis for SF was performed using the whole population, Sub1, and Sub2, respectively.

With 1000 permutation tests ($p < 0.05$), the threshold of SF QTL in the five trials ranged from 1.5 to 2.4. To exclude false positive QTL, the score of 2.4 was set as the *LOD* threshold (Table 3). Six QTL for SF were detected in the whole population. Five of them showed significant effects on SD4, the last sowing trial in 2020. QTL *qSF8* located in the *DTH8* region had the highest and second highest R^2, i.e., 34.6% on SD4 and 28.9% on SD3. This QTL was also detected on SD2 but the R^2 value decreased to 8.1%. The allele for increasing SF was from ZH161, which carries the non-functional *DTH8* allele. The effect became nonsignificant in the two early-sowing trials, i.e., the only trial in 2019 and the SD1 trial in 2020.

Table 3. QTL for spikelet fertility detected in the D71/ZH161 RIL population.

QTL	Interval [a]	Trial	Whole Population			Sub1 [d]			Sub2 [e]		
			LOD	*A* [b]	R^2 (%) [c]	*LOD*	*A*	R^2 (%)	*LOD*	*A*	R^2 (%)
qSF1	1_40679–1_40748	2020-SD4	3.4	2.1	2.9	-	-	-	-	-	-
qSF2	2_22510–2_26472	2019	4.8	1.8	7.7	-	-	-	-	-	-
		2020-SD1	3.5	1.4	4.8	-	-	-	-	-	-
		2020-SD2	2.9	1.2	4.3	-	-	-	-	-	-
		2020-SD3	2.5	1.4	2.9	-	-	-	-	-	-
		2020-SD4	2.5	1.7	2.1	-	-	-	-	-	-
qSF3.1	3_894–3_1306	2020-SD4	6.6	−3.0	6.2	5.7	−5.1	17.3	-	-	-
qSF3.2	3_16442–3_17745	2019	5.6	1.9	9.2	-	-	-	-	-	-
		2020-SD1	12.3	2.7	18.5	7.3	3.1	20.1	-	-	-
		2020-SD2	8.9	2.2	14.0	7.8	3.4	22.6	-	-	-
		2020-SD3	7.7	2.6	9.5	4.5	3.4	15.5	-	-	-
		2020-SD4	4.8	2.5	4.2	-	-	-	-	-	-
qSF8	8_3570–8_4554	2020-SD2	5.3	1.7	8.1	-	-	-	-	-	-
		2020-SD3	20.7	4.5	28.9	-	-	-	-	-	-
		2020-SD4	30.9	7.0	34.6	-	-	-	-	-	-
qSF11	11_19486–11_24346	2020-SD1	3.6	1.4	5.0	-	-	-	-	-	-
		2020-SD3	-	-	-	-	-	-	3.6	1.7	13.2
		2020-SD4	-	-	-	-	-	-	3.5	1.7	12.4
qSF7	7_24670–7_24670	2020-SD2	-	-	-	-	-	-	3.1	1.5	11.8
qSF10	10_5369–10_9088	2020-SD1	-	-	-	2.6	−1.8	6.7	-	-	-

[a] An interval is indicated by the two markers flanking the QTL. An SNP marker is named the chromosome No. followed by the physical position in kb. [b] *A*, additive effect of replacing a maternal allele with a paternal allele. Positive values indicate that alleles from ZH161 are in the direction of increasing the trait score, and negative values indicate that alleles from D71 are in the direction of increasing the score. [c] R^2, the proportion of phenotypic variance explained by the QTL effect. [d] Sub1, the subpopulation containing 133 lines carrying the functional $DTH8^{D71}$ allele. [e] Sub 2, the subpopulation containing 120 lines carrying the non-functional $DTH8^{ZH161}$ allele.

The third and fourth largest R^2, 18.5% and 14.0%, were occupied by *qSF3.2* on SD1 and SD2, respectively. In addition, this QTL was detected in the other three trials, with the R^2 values ranging from 4.2% to 9.5%. Another QTL, *qSF2*, was also detected in all five trials, with R^2 values ranging from 2.1% to 7.7%. The alleles for increasing SF in the two QTL regions were both derived from ZH161. In the two subpopulations, *qSF2* showed no significant effects, while *qSF3.2* was detected on SD1, SD2, and SD3 trials in the Sub1 population, in which the RILs may have suffered from high-temperature stress.

Two other QTL were detected in the whole population. *qSF1* and *qSF3.1* were detected on SD4 only, with R^2 values of 2.9% and 6.2% in the alleles for increasing SF derived from ZH161 and D71, respectively. Moreover, *qSF3.1* was also detected in the SD4 trial in the Sub1 population, in which the RILs suffered greatly from high-temperature stress. Its additive effect and R^2 were much larger in the Sub1 population than the whole population (Table 3). The last QTL showing a significant effect in the whole population, *qSF11*, which was detected on SD1 only. This QTL showed no significant effects in the Sub1 population but was detected in the Sub2 population in two of the four trials conducted in 2020.

Two other QTL, *qSF7* and *qSF10*, were not detected in the whole population but were detected in the SD2 trial in the Sub2 population and the SD1 trial in the Sub1 population, respectively. They were detected with *LOD* scores of 3.1 and 2.6, additive effects of 1.5% and 1.8%, and R^2 values of 11.8% and 6.7%, and the alleles for increasing SF were derived from ZH161 and D71, respectively.

In addition, as shown in Figure 2, SF shows a similar variation trend between SD1 and SD2, and between SD3 and SD4, respectively. Therefore, the homogeneity of variance was tested in these two groups. The result showed that equal variance was only detected between SD1 and SD2 (p = 0.318). To further compare the QTL region in each trial, QTL analysis for SF in the whole population was performed using the recombinant data on

SD1 and SD2, and SD3 and SD4, respectively. As shown in Table S2, five QTL for SF were detected. Four of them, *qSF2*, *qSF3.1*, *qSF3.2*, and *qSF8*, were still detected. One QTL, *qSF5*, was newly detected with *LOD* scores of 3.7, additive effects of 1.6%, and R^2 values of 2.9%. The four QTL *qSF2*, *qSF3.1*, *qSF3.2*, and *qSF8* were commonly detected from different groups, indicating that these four regions had high reliability.

4. Discussion

With global warming, rice production is facing more and more abiotic stresses, such as high temperatures, low temperatures, and drought stress [38], among which high-temperature damage has become a bottleneck affecting rice growth and development. The decrease in rice spikelet fertility caused by high temperatures has become one of the main reasons restricting rice production safety [39]. Exploring QTL for improving spikelet fertility under high-temperature stress is of great importance for the improvement of rice varieties with high-temperature tolerance. In this study, five QTL-controlling SF associated with high-temperature tolerance were identified using a high-density linkage map. The *qSF8* was located in the *DTH8* region, which showed a major effect on SF under high-temperature stress. However, it explained a much smaller proportion of SF variance compared with its contribution to HD. So, is it because the extension of the heading date indirectly affects the spikelet fertility after encountering high-temperature stress, or does the gene itself control the effect of high-temperature stress on spikelet fertility? Further study is pending. Two QTL, *qSF2* and *qSF3.2*, were detected in all five trials. The ZH161 alleles at both QTL can increase spikelet fertility under normal temperatures or high-temperature stress. The remaining two QTL, *qSF1* and *qSF3.1*, were detected only in the SD4 trial, in which the RILs suffered greatly from high-temperature stress. Both of them had no significant effect on SF at normal temperature but showed significant effects under high-temperature stress, especially *qSF3.1*, whose additive effect and R^2 were much larger in the Sub1 population than the whole population. These QTL have an important potential in improving rice variety with high-temperature tolerance.

Given that the *qSF8* is clearly in the *DTH8* region, the genomic positions of the remaining four QTL were compared with published heat-tolerant QTL. *qSF1* was located in the interval of 1_40679-1_40748, corresponding to the 40.6–40.7 Mb region on chromosome 1 in the Nipponbare genome. Two previous studies have also detected QTL for spikelet fertility under high-temperature stress close to this position. The *qHTSf1.1* reported by Ye et al. [40] was located close to the SNP id1023892, which corresponds to the 39.6 Mb on chromosome 1. The *qHTB1* reported by Zhu et al. [41] was located in the interval of RM1387-RM8137, which corresponds to the 40.2–42.9 Mb region. Likewise, *qSF2*, *qSF3.1*, and *qSF3.2* were located in the intervals of 2_22510-2_26472, 3_894-3_1306, and 3_16442-3_17745, respectively, which correspond to the 22.5–26.4 Mb region on chromosome 2, and the 0.8–1.3 Mb and 16.4–17.7 Mb regions on chromosome 3, respectively. Correspondingly, the *qHt2* controlling the seed-setting rate reported by Chen et al. [42], and the *qHTB3-1* and *qHTB3-2* controlling spikelet fertility reported by Zhu et al. [41], were located in the intervals of RM183-RM106, RM4108, and RM5748-RM5864, which correspond to the 25.1–29.3 Mb region on chromosome 2 and 0.54 Mb and 12.3–22.3 Mb on chromosome 3, respectively. Consistent detection of these QTL in different genetic backgrounds suggests that these regions are highly reliable and provide candidate regions for gene cloning.

It is well-known that plants generally perceive and integrate diverse environmental cues to determine the appropriate timing of the phase transition to maximize reproductive success, or rapidly induce flowering before stress becomes a large detrimental factor or temporarily inhibit heading until stress has passed [43]. The rice heading date is generally regarded as a key indicator of the response to temperature variation. Earlier studies suggested that the heading date genes/pathways in rice may play an important role in the integration of the floral transition and the high-temperature stress response. *qHd1*/*OsMADS51*, a QTL with a minor effect on the heading date in rice, regulated heading in response to temperature and contributed to high-temperature tolerance at the heading and grain

filling stages. Transcriptome profiling revealed that the *qHd1-Ehd1-RFT1/Hd3a* pathway is the basis for *qHd1*-mediated flowering response to temperature [23]. Likewise, the *Ghd7* transcript was regulated by various environmental signals such as high temperatures, cold temperatures, and drought, and the expression level of *Ghd7* subsequently regulated the growth and development of the rice plant to escape or avoid stresses [25,44]. In this study, as shown in Figures 2 and S1, the Sub2 population carrying the non-functional *dth8* allele had a high SF at all four sowing dates, and its heading date was significantly earlier than the Sub1 population carrying the functional *DTH8* allele. The response of *qHd1* and *Ghd7* to environmental stress provides a theoretical basis for the function of *DTH8* in avoiding high-temperature stress by heading early. This regulation mechanism needs further study.

Genetic drag is a common obstacle in rice breeding [45]. In this study, we found that two regions showed an unfavorable linkage between heading date and spikelet fertility, i.e., *qHD1/qSF1* and *qHD8/qSF8*. The allele from female parent D71 increased heading date but reduced spikelet fertility. Especially at *qHD8/qSF8*, with the delay of the sowing date, the negative effect of the D71 allele on spikelet fertility was greater. The additive effect values were 1.7%, 4.5%, and 7.0% on SD2, SD3, and SD4, respectively (Table 3). On the contrary, at the *qHD3/qSF3.1* region, the allele from D71 promoted heading and increased spikelet fertility. These results suggested that *qHD3/qSF3.1* may alleviate the genetic drag of the above two regions, especially under high-temperature stress.

5. Conclusions

In this study, RILs derived from an *indica* rice cross between two restorer lines of three-line hybrid rice were used to identify QTL for HD and SF that were related to high-temperature tolerance. For HD, a total of six QTL were detected. All of them corresponded in position to the cloned genes, among which *qHD8* in the *DTH8/Ghd8* region showed the largest genetic effect. For SF, a total of eight QTL were detected. Five of them, *qSF1*, *qSF2*, *qSF3.1*, *qSF3.2*, and *qSF8*, showed high-temperature tolerance and had an important potential in rice breeding.

Supplementary Materials: The following supporting information can be downloaded at https://www.mdpi.com/article/10.3390/agronomy13061582/s1. Table S1: The primers used in this study. Table S2: Detection of QTL for spikelet fertility by recombinant data of the D71/ZH161 RIL population at different sowing dates. Figure S1: Spikelet fertility of each line in subpopulation 1 and subpopulation 2 in the four sowing dates.

Author Contributions: Conceptualization, J.Z., S.T. and Y.Z.; methodology, D.H. and Z.Z.; investigation, D.H. and Y.F.; data curation, J.Z. and Y.Z.; writing—original draft preparation, D.H., J.Z. and Y.Z.; writing—review and editing, J.Z. and Y.Z. All authors have read and agreed to the published version of the manuscript.

Funding: This research was funded by the Outstanding Talents for Ten Thousand Talents Program of Zhejiang Province (2020R51007), the Agricultural Science and Technology Innovation Program (CAAS-ASTIP-2021-CNRRI), and the Central Public-interest Scientific Institution Basal Research Fund (CPSIBRF-CNRRI-202112).

Data Availability Statement: Not applicable.

Conflicts of Interest: The authors declare no conflict of interest.

References

1. Li, J.-Y.; Yang, C.; Xu, J.; Lu, H.-P.; Liu, J.-X. The hot science in rice research: How rice plants cope with heat stress. *Plant Cell Environ.* **2022**, *46*, 1087–1103. [CrossRef]
2. Ye, C.; Tenorio, F.A.; Argayoso, M.A.; Laza, M.A.; Koh, H.-J.; Redona, E.D.; Jagadish, K.S.V.; Gregorio, G.B. Identifying and confirming quantitative trait loci associated with heat tolerance at flowering state in different rice populations. *BMC Genet.* **2015**, *16*, 41. [CrossRef] [PubMed]
3. Prasad, P.V.V.; Bheemanahalli, R.; Jagadish, S.V.K. Field crops and the fear of heat stress-Opportunities, challenges and future directions. *Field Crop. Res.* **2017**, *200*, 114–121. [CrossRef]

4. Chen, L.; Wang, Q.; Tang, M.; Zhang, X.; Pan, Y.; Yang, X.; Gao, G.; Lv, R.; Tao, W.; Jiang, L.; et al. QTL mapping and identification of candidate genes for heat tolerance at the flowering stage in rice. *Front. Genet.* **2021**, *11*, 621871. [CrossRef]
5. Xiong, D.; Ling, X.; Huang, J.; Peng, S. Meta-analysis and dose-response analysis of high temperature effects on rice yield and quality. *Environ. Exp. Bot.* **2017**, *141*, 1–9. [CrossRef]
6. Qin, P.; Zhang, G.; Hu, B.; Wu, J.; Chen, W.; Ren, Z.; Liu, Y.; Xie, J.; Yuan, H.; Tu, B.; et al. Leaf-derived ABA regulates rice seed development via a transporter-mediated and temperature-sensitive mechanism. *Sci. Adv.* **2021**, *7*, 8873. [CrossRef]
7. Stocher, T.F.; Plattner, G.K.; Tignor, M.M.B.; Allen, S.K.; Boschung, J.; Nauel, A.; Xia, Y.; Bex, V.; Midgley, P. *Climate Change 2013: The Physical Science Basis: Working Group I Contribution to the Fifth Assessment Report of the Intergovernmental Panel on Climate Change*; Cambridge University Press: Cambridge, UK, 2013.
8. Zhao, C.; Liu, B.; Piao, S.; Wang, X.; Lobell, D.B.; Huang, Y.; Huang, M.; Yao, Y.; Bassu, S.; Ciais, P.; et al. Temperature increase reduces global yields of major crops in four independent estimates. *Proc. Natl. Acad. Sci. USA* **2017**, *114*, 9326–9331. [CrossRef]
9. Kan, Y.; Lin, H.-X. Molecular regulation and genetic control of rice thermal response. *Crop. J.* **2021**, *9*, 497–505. [CrossRef]
10. Kilasi, N.L.; Singh, J.; Vallejos, C.E.; Ye, C.; Jagadish, S.V.K.; Kusilwa, P.; Rathinasabapathi, B. Heat stress tolerance in rice (*Oryza sativa* L.): Identification of quantitative trait loci and candidate genes for seeding growth under heat stress. *Front. Plant Sci.* **2018**, *9*, 1578. [CrossRef] [PubMed]
11. Park, J.-R.; Yang, W.-T.; Kim, D.-H.; Kim, K.-M. Identification of a novel gene, *Osbht*, in responese to high temperature tolerance at booting stage in rice. *Int. J. Mol. Sci.* **2020**, *21*, 5862. [CrossRef]
12. Zhang, C.; Chen, F.; Hong, R.; Li, Q.; Gu, M.; Liu, Q. Mapping QTLs for heat tolerance in rice (*Oryza sative* L.) at heading stage using chromosome segment substitution lines. *Agric. Biotechnol.* **2017**, *6*, 15–18.
13. Wada, T.; Miyahara, K.; Sonoda, J.-Y.; Tsukaguchi, T.; Miyazaki, M.; Tsubone, M.; Ando, T.; Ebana, K.; Yamamoto, T.; Norio, I.; et al. Deteceion of QTLs for white-back and basal-white grains caused by hihg temperature during ripening period in *japonica* rice. *Breed. Sci.* **2015**, *65*, 216–225. [CrossRef]
14. Xu, Y.; Chu, C.; Yao, S. The impact of high-temperature stress on rice: Challenges and solutions. *Crop. J.* **2021**, *9*, 963–976. [CrossRef]
15. Li, X.-M.; Chao, D.-Y.; Wu, Y.; Huang, X.; Chen, K.; Gui, L.-G.; Su, L.; Ye, W.-W.; Chen, H.; Chen, H.-C.; et al. Natural alleles of a proteasome α2 subunit gene contribute to thermotolerance and adaptation of African rice. *Nat. Genet.* **2015**, *47*, 827–836. [CrossRef] [PubMed]
16. Kan, Y.; Mu, X.-R.; Zhang, H.; Gao, J.; Shan, J.-X.; Ye, W.-W.; Lin, H.-X. *TT2* controls rice thermotolerance through SCT1-dependent alteration of wax biosynthesis. *Nat. Plants* **2022**, *8*, 53–57. [CrossRef]
17. Zhang, H.; Zhou, J.-F.; Shan, J.-X.; Ye, W.-W.; Dong, N.-Q.; Guo, T.; Xiang, Y.-H.; Yang, Y.-B.; Li, Y.-C.; Zhao, H.-Y. A genetic module at one locus in rice protects chloroplasts to enhance thermotolerance. *Science* **2022**, *376*, 1293–1300. [CrossRef]
18. Cao, Z.; Li, Y.; Tang, H.; Zeng, B.; Tang, X.; Long, Q.; Wu, X.; Cai, Y.; Yuan, L.; Wan, J. Fine mapping of the *qHTB1-1*QTL, which confers heat tolerance at the booting stage, using an *Oryza rufipogon* Griff. Introgression line. *Theor. Appl. Genet.* **2020**, *133*, 1161–1175. [CrossRef]
19. Shen, H.; Zhong, X.; Zhao, F.; Wang, Y.; Yan, B.; Li, Q.; Chen, G.; Mao, B.; Wang, J.; Li, Y.; et al. Overexpression of receptor-like kinase *ERECTA* improves thermotolerance in rice and tomato. *Nat. Biotechnol.* **2015**, *33*, 996–1003. [CrossRef] [PubMed]
20. Liu, J.; Zhang, C.; Wei, C.; Liu, X.; Wang, M.; Yu, F.; Xie, Q.; Tu, J. The ring finger ubiquitin E3 ligase OsHTAS enhances heat tolerance by promoting H_2O_2-induced stomatal closure in rice. *Plant Physiol.* **2016**, *170*, 429–443. [CrossRef]
21. Qiu, Z.; Kang, S.; He, L.; Zhao, J.; Zhang, S.; Hu, J.; Zeng, D.; Zhang, G.; Dong, G.; Gao, Z.; et al. The newly identified *heat-stress sensitive albino 1* gene affects chloroplast development in rice. *Plant Sci.* **2018**, *267*, 168–179. [CrossRef]
22. Zhu, Y.-J.; Fan, Y.-Y.; Wang, K.; Huang, D.-R.; Liu, W.-Z.; Ying, J.-Z.; Zhuang, J.-Y. *Rice flowering locus T1* plays an important role in heading date influencing yield traits in rice. *Sci. Rep.* **2017**, *7*, 4718.
23. Chen, J.-Y.; Zhang, H.-W.; Zhang, H.-L.; Ying, J.-Z.; Ma, L.-Y.; Zhuang, J.-Y. Natural variation at *qHd1* affects heading date acceleration at high temperatures with pleiotropism for yield traits in rice. *BMC Plant Biol.* **2018**, *18*, 112. [CrossRef] [PubMed]
24. Zhang, Z.; Zhu, Y.; Wang, S.; Fan, Y.; Zhuang, J. Genetic interaction of *Hd1* with *Ghd7*, *DTH8* and *Hd2* largely determines eco-geographical adaption of rice varieties in southern China. *Rice Sci.* **2021**, *28*, 114–118.
25. Weng, X.; Wang, L.; Wang, J.; Hu, Y.; Du, H.; Xu, C.; Xing, Y.; Li, X.; Xiao, J.; Zhang, Q. Grain number, plant height, and heading date 7 is a central regulator of growth, development, and stress response. *Plant Physiol.* **2014**, *164*, 735–747. [CrossRef]
26. Kazan, K.; Lyons, R. The link between flowering time and stress tolerance. *J. Exp. Bot.* **2016**, *67*, 47–60. [CrossRef]
27. Zhang, C.; Li, G.; Chen, T.; Feng, B.; Fu, W.; Yan, J.; Islam, M.R.; Jin, Q.; Tao, L.; Fu, G. Heat stress induces spikelet sterility in rice at anthesis through inhibition of pollen tube elongation interfering with auxin homeostasis in pollinated pistils. *Rice* **2018**, *11*, 14. [CrossRef]
28. Kanyange, L.; Fan, Y.-Y.; Zhang, Z.-H.; Huang, D.-R.; Huang, T.-X.; Zhuang, J.-Y. Genetic association between blast resistance and yield traits in rice detected using a high-density bin map. *Agronomy* **2022**, *12*, 1173. [CrossRef]
29. Meng, L.; Li, H.; Zhang, L.; Wang, J. QTL IciMapping: Integrated software for genetic linkage map construction and quantitative trait locus mapping in biparental populations. *Crop. J.* **2015**, *3*, 269–283. [CrossRef]
30. McCouch, S.R. CGSNL (Committee on Gene Symbolization, Nomenclature and Linkage, Rice Genetics Cooperative). Gene nomenclature system for rice. *Rice* **2008**, *1*, 72–84. [CrossRef]

31. Wei, X.; Xu, J.; Guo, H.; Jiang, L.; Chen, S.; Yu, C.; Zhou, Z.; Hu, P.; Zhai, H.; Wan, J. *DTH8* suppresses flowering in rice, influencing plant height and yield potential simultaneously. *Plant Physiol.* **2010**, *153*, 1747–1758. [CrossRef]
32. Yan, W.-H.; Wang, P.; Chen, H.-X.; Zhou, H.-J.; Li, Q.-P.; Wang, C.-R.; Ding, Z.-H.; Zhang, Y.-S.; Yu, S.-B.; Xing, Y.-Z.; et al. A major QTL, *Ghd8*, plays pleiotropic roles in regulating grain productivity, plant height, and heading date in rice. *Mol. Plant* **2010**, *4*, 319–330. [CrossRef] [PubMed]
33. Kim, S.L.; Lee, S.; Kim, H.J.; Nam, H.G.; An, G. *OsMADS51* is a short-day flowering promoter that functions upstream of *Ehd1*, *OsMADS14*, and Hd3a. *Plant Physiol.* **2007**, *145*, 1484–1494. [CrossRef] [PubMed]
34. Bian, X.F.; Liu, X.; Zhao, Z.G.; Jiang, L.; Gao, H.; Zhang, Y.H.; Zhang, M.; Chen, L.M.; Liu, S.J.; Zhai, H.Q.; et al. Heading date gene, *dth3* controlled late flowering in *O.Glaberrima* Steud. by down-regulating *Ehd1*. *Plant Cell Rep.* **2011**, *30*, 2243–2254. [CrossRef]
35. Yano, M.; Katayose, Y.; Ashikari, M.; Yamanouchi, U.; Monna, L.; Fuse, T.; Baba, T.; Yamamoto, K.; Umehara, Y.; Nagamura, Y.; et al. *Hd1*, a major photoperiod sensitivity quantitative trait locus in rice, is closely related to the arabidopsis flowering time gene *CONSTANS*. *Plant Cell* **2000**, *12*, 2473–2483. [CrossRef] [PubMed]
36. Sun, B.; Zhan, X.-D.; Lin, Z.-C.; Wu, W.-X.; Yu, P.; Zhang, Y.-X.; Sun, L.-P.; Cao, L.-Y.; Cheng, S.-H. Fine mapping and candidate gene analysis of *qHD5*, a novel major QTL with pleiotropism for yield-related traits in rice (*Oryza sativa* L.). *Theor. Appl. Genet.* **2017**, *130*, 247–258. [CrossRef] [PubMed]
37. Yan, W.; Liu, H.; Zhou, X.; Li, Q.; Zhang, J.; Lu, L.; Liu, T.; Liu, H.; Zhang, C.; Zhang, Z.; et al. Natural variation in *Ghd7.1* plays an important role in grain yield and adaptation in rice. *Cell Res.* **2013**, *23*, 969–971. [CrossRef]
38. Dar, M.H.; Bano, D.A.; Waza, S.A.; Zaidi, N.W.; Majid, A.; Shikari, A.B.; Ahangar, M.A.; Hossain, M.; Kumar, A.; Singh, U.S. Abiotic stress tolerance-progress and pathways of sustainable rice production. *Sustainability* **2021**, *13*, 2078. [CrossRef]
39. Wang, Y.; Wang, L.; Zhou, J.; Hu, S.; Chen, H.; Xiang, J.; Zhang, Y.; Zeng, Y.; Shi, Q.; Zhu, D.; et al. Research progress on heat stress of rice at flowering stage. *Rice Sci.* **2019**, *26*, 1–10. [CrossRef]
40. Ye, C.; Argayoso, M.; Redona, E.D.; Sierra, S.N.; Laza, M.; Dilla, C.; Mo, Y.; Thomson, M.J.; Chin, J.; Delavina, C.B.; et al. Mapping QTL for heat tolerance at flowering stage in rice using SNP markers. *Plant Breed.* **2012**, *131*, 33–41. [CrossRef]
41. Zhu, S.; Huang, R.; Wai, H.P.; Xiong, H.; Shen, X.; He, H.; Yan, S. Mapping quantitative trait loci for heat tolerance at the booting stage using chromosomal segment substitution lines in rice. *Physiol. Mol. Biol. Plant* **2017**, *23*, 817–825. [CrossRef]
42. Chen, Q.-Q.; Yu, S.-B.; Li, C.-H.; Mou, T.-M. Identification of QTLs for heat tolerance at flowering stage in rice. *Sci. Agric. Sinaca* **2008**, *41*, 315–321, (In Chinese with English Abstract).
43. Andres, F.; Coupland., G. The genetic basis of flowering responses to seasonal cues. *Nat. Rev. Genet.* **2012**, *13*, 627. [CrossRef] [PubMed]
44. Xue, W.; Xing, Y.; Weng, X.; Zhao, Y.; Tang, W.; Wang, L.; Zhou, H.; Yu, S.; Xu, C.; Li, X.; et al. Natural variation in *Ghd7* is an important regulator of heading date and yield potential in rice. *Nat. Genet.* **2008**, *40*, 761–767. [CrossRef] [PubMed]
45. Wei, X.; Qiu, J.; Yong, K.; Fan, J.; Zhang, Q.; Hua, H.; Liu, J.; Wang, Q.; Olsen, K.M.; Han, B.; et al. A quantitative genomics map of rice provides genetic insights and guides breeding. *Nat. Genet.* **2021**, *53*, 243–256. [CrossRef]

Disclaimer/Publisher's Note: The statements, opinions and data contained in all publications are solely those of the individual author(s) and contributor(s) and not of MDPI and/or the editor(s). MDPI and/or the editor(s) disclaim responsibility for any injury to people or property resulting from any ideas, methods, instructions or products referred to in the content.